Supplementary information

An investigation of two copper(II) complexes with a triazole derivative as a ligand: magnetic and catalytic properties

Yuliia P. Petrenko,[a] Karolina Piasta,[d] Dmytro M. Khomenko,[a*] Roman O. Doroshchuk,[a] Sergiu Shova,[b] Ghénadie Novitchi,[c] Yuliya Toporivska,[d] Elzbieta Gumienna-Kontecka,[d**] Luísa M. D. R. S. Martins[e***] and Rostyslav D. Lampeka[a]

[a] Department of Chemistry, Taras Shevchenko National University of Kyiv, Volodymyrska Street, 64/13, Kyiv 01601, Ukraine

[b] "Petru Poni" Institute of Macromolecular Chemistry, Laboratory of Inorganic Polymers, Aleea Grigore Ghica Voda No. 41A, RO-700487 Iasi, Romania

[c] Laboratoire National des Champs Magnétiques Intenses, UPR CNRS 3228, Université Grenoble-Alpes, 25 rue des Martyrs, B.P. 166, 38042 Grenoble Cedex 9, France

[d] Faculty of Chemistry, University of Wroclaw, F. Joliot-Curie 14, 50-383 Wroclaw, Poland

[e] Centro de Química Estrutural and Departamento de Engenharia Química, Instituto Superior Técnico, Universidade de Lisboa, Av. Rovisco Pais, 1049-001 Lisboa, Portugal

Corresponding author*. Tel.: +380 50 548 6005; fax: +380 44 490 7185.
E-mail address: dkhomenko@ukr.net (Dmytro M. Khomenko),
Corresponding author**. Tel.: +48 71 3757251.
E-mail address: elzbieta.gumienna-kontecka@chem.uni.wroc.pl (Elzbieta Gumienna-Kontecka).
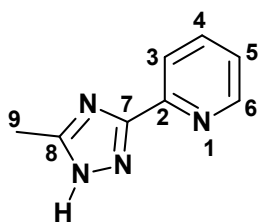Corresponding author***.
E-mail address: luisammartins@tecnico.ulisboa.pt (Luísa M.D.R.S. Martins)

Contents

SPECTROSCOPIC CHARACTERIZATION

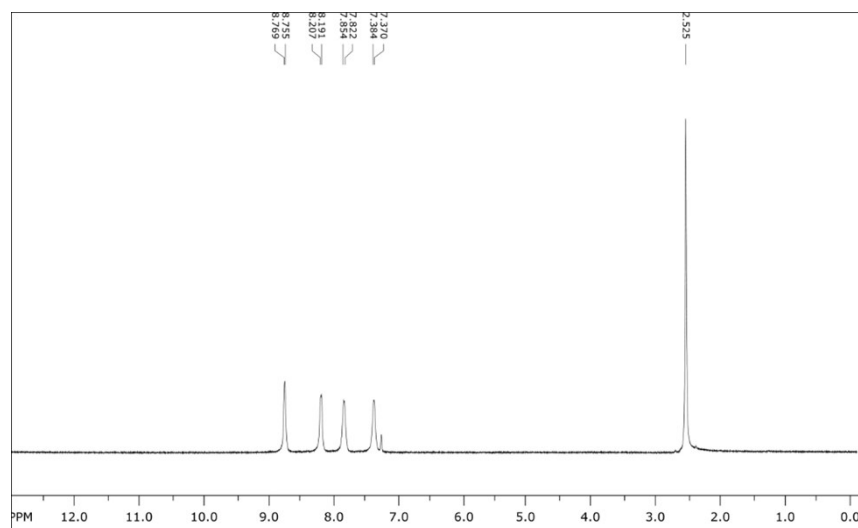## NMR spectroscopy

3-(2-pyridyl)-5-methyl-1,2,4-triazole (HL)

Figure S1. ^{1}H NMR spectrum of HL**(400 MHz, CDCl$_3$)**: δ [ppm] = 8.76 (d, $^3J_{H,H}$ = 4.6 Hz, 1H, Py-H^6), 8.20 (d, $^3J_{H,H}$ = 7.7 Hz 1H, Py-H^3), 7.84 (t, $^3J_{H,H}$ = 7.8 Hz 1H, Py-H^4), 7.38 (t, $^3J_{H,H}$ = 7.5 Hz, 1H, Py-H^5), 2.53 (s, 3H, H^9).

IR spectroscopy
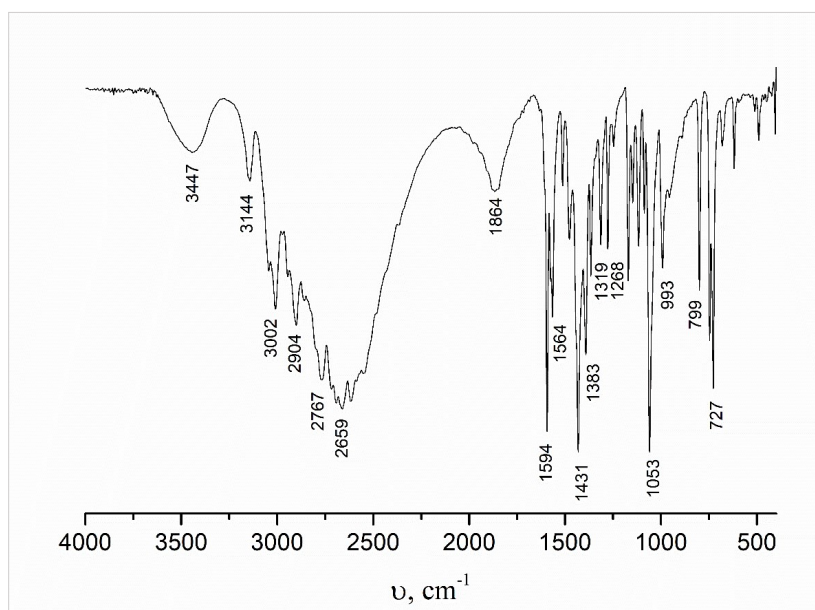
Figure S2 (1). IR of ligand HL: ν [cm^{-1}] = 3447 (w), 3144 (w), 3002 (m), 2904 (m), 2767 (m), 2659 (m), 1864 (w), 1594 (s), 1564 (m), 1431 (s), 1383 (m), 1319 (s), 1268 (s), 1053 (s), 993 (m), 799 (s), 727 (s).

IR spectroscopy

Figure S2 (2). IR of complex **1**: ν [cm⁻¹] = 3381 (m), 3231 (m), 3072 (w), 1671 (w), 1581 (s), 1474 (m), 1402 (s), 1336 (m), 1143 (m), 1018 (w), 757 (s), 674 (s).

Figure S2 (3). IR of complex **2**: ν [cm⁻¹] = 3058 (s), 3024 (w), 2925 (m), 2853 (w), 1658 (m), 1600 (s), 1530 (s), 1466 (m), 1290 (m), 1250 (m), 1125 (s), 1026 (m), 791 (s), 748 (s), 709 (s), 641 (s).

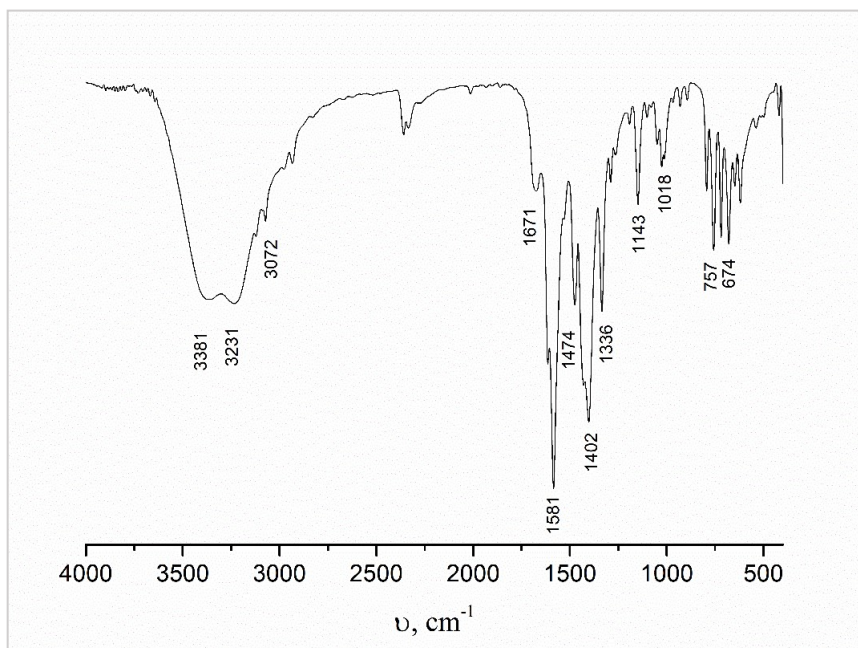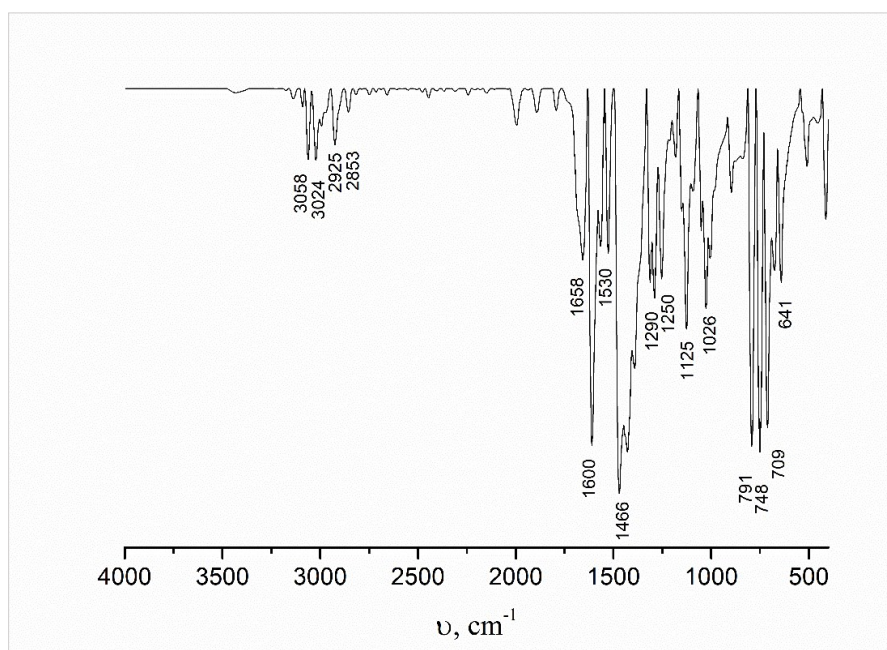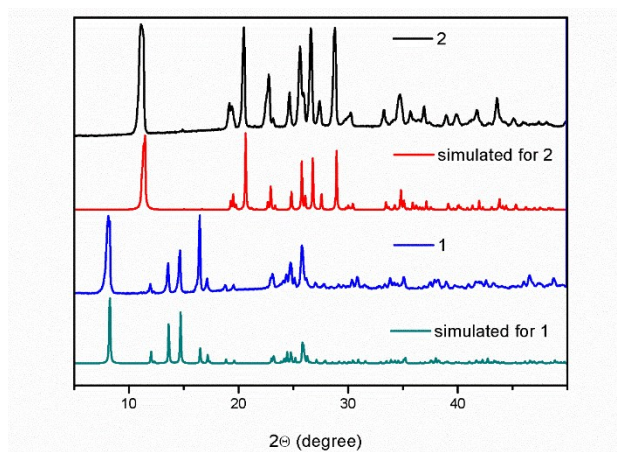*PXRD measurements*

Figure S3. The comparisons for the PXRD profiles for the complexes **1** and **2.**

EXPERIMENTAL PROCEDURES

Refinement X-ray crystallography

X-ray diffraction data for **1**, **2** were collected with an Oxford-Diffraction XCALIBURE CCD diffractometer equipped with graphite-monochromated Mo$K\alpha$ radiation. The experimental data comprises 305 and 219 frames each for 30 and 10 s over 1° oscillation width and crystal-to-detector distance at 40 mm. The unit cell determination and data integration were carried out using the CrysAlis package of Oxford Diffraction.[1] The structure was solved by direct methods using Olex2[2] software with the SHELXS structure solution program and refined by full-matrix least-squares on F^2 with SHELXL-2015.[3] Hydrogen atoms were inserted in fixed, idealized positions and refined as rigidly bonded to the corresponding atoms. The positional parameters for H-atoms of water molecules were determined from Fourier maps and refined according to H-bonds parameters. The molecular plots were obtained using the Olex2 program. Crystal data and some further details concerning X-ray analysis are given in Table 3. The bonds lengths and angles are listed in Table S4-6, CCDC-2008470, 2008469. These data can be obtained free of charge via www.ccdc.cam.ac.uk/conts/retrieving.html (or from the Cambridge Crystallographic Data Centre, 12 Union Road, Cambridge CB2 1EZ, UK; fax: (+44) 1223-336-033; or deposit@ccdc.ca.ac.uk).

Magnetic measurements

Magnetic measurements for [Cu$_2$(L)$_2$(OAc)$_2$(H$_2$O)$_2$] (**1**) were carried out on microcrystalline sample with a Quantum Design SQUID magnetometer (MPMS-XL). Variable-temperature (2-300 K) direct current magnetic susceptibility was measured under an applied magnetic field of 0.1 T. All data were corrected for the contribution of the sample holder and diamagnetism of the samples estimated from Pascal's constants.[4] The analysis of the magnetic data was carried out by a simultaneous fit of the $\chi_M T(T)$ and $\chi_M(T)$ thermal variations including temperature independent paramagnetism (*TIP*), impurity contribution (ρ), and intermolecular interaction (z*J'*)[5] according to the expression:

$$\chi_M(T) = \frac{\chi_d(T)}{\left[1 - \frac{2zJ'\chi_d(T)}{Ng^2\beta^2}\right]}(1-\rho) + \rho\frac{Ng^2\beta^2}{3kT}S(S+1) + TIP$$

Physical measurements

Potentiometric titrations of HL and its complexes with copper(II) ions were performed using Titrando 905 (Metrohm) automatic titrator system. The combined glass electrode (Mettler Toledo InLab Semi-Micro) was filled with 0.1M NaCl in MeOH/H$_2$O (80:20 w/w) ionic strength and conditioned for two weeks before the first measurements were made, and was stored in the same electrolyte solution between measurements. The daily calibration of the electrode in hydrogen ion concentration was performed using HNO$_3$. The experiments were carried out on 3ml samples with the ligand concentration of 1·10^{-3} M and copper(II) to ligand molar ratios 1:1 and 1:3 under argon atmosphere at 25±0.2°C. The exact concentration of the ligand was determined using the Gran method.[6] The obtained potentiometric data were refined with Superquad program[7], using nonlinear least-squares methods.[8] The pKw in the solvent mixture used in calculations was -14.42.[9]

Absorption spectra were recorded on a Varian CARY 300 UV-Vis spectrophotometer. pH-dependent UV-Vis titrations were performed in the pH range 2-10 at 25.0±0.2 °C using the combined glass electrode (Mettler Toledo InLab Semi-Micro) prepared as in the case of potentiometric titrations and calibrated with buffers prepared in MeOH/H$_2$O mixture (80:20 w/w)[10,11] before every measurement. The starting pH was adjusted to around 2 with HNO$_3$ and the titration was carried out in a cell with 1 cm optical path length with 3 ml as total volume of the solution containing 1:1 and 1:3 molar ratios of Cu(II):ligand with the concentration of the ligand around 1·10^{-3} M.

EPR spectra were recorded using a Bruker ELEXSYS E500 CW-EPR spectrometer equipped with frequency counter (E 41 FC) at 77K at X-band frequency and an NMR teslameter (ER 036TM). The solutions for EPR were prepared by using MeOH/H$_2$O mixture (80/20 w/w). The parameters of experimental spectra were determined by spectra simulation in Doublet new (EPR OF S=1/2) program by Dr. Andrew Ozarowski, National High Field Magnetic Laboratory, University of Florida.

Electrospray ionization mass spectrometry (ESI-MS) data were collected on a Bruker apex ultra FT-ICR mass spectrometer (Bruker Daltonik, Germany), equipped with an Apollo II electrospray ionization source with an ion funnel. The instrument parameters were: dry gas– nitrogen, temperature 200°C, ion source voltage 4500 V, collision energy 10 eV. The instrument was calibrated using the Tunemix mixture (Bruker Daltonik, Germany) in the

quadratic regression mode. The spectra were recorded in the positive ion mode in the range 100 to 1500 m/z. The stock solutions were prepared by using MeOH/H$_2$O mixture (80/20 w/w) as a solvent. Copper (II) to ligand molar ratios were 1:1 and 1:3 and the final pH of the solutions was 8. MS spectra were analyzed on a Bruker Compass Data Analysis 4.0 software and the overall charge of the analyzed ion was calculated on the base of the distance between the isotopic peaks.

Catalytic studies

The oxidations of styrene and of cyclohexane were performed under microwave irradiation (15 and 10 W, respectively) in a focused microwave Anton Paar Monowave 300 discover reactor fitted with a rotational system and an IR temperature detector. A 10 mL capacity cylindrical Pyrex tube with a 13 mm internal diameter was used.

For a typical oxidation of styrene: complex **1** or **2** (10.0 μmol), styrene (1.0 mmol), hydrogen peroxide (30% w/w aq. sol., 2.0 mmol), 1 mL of acetonitrile and 100 μL of chlorobenzene (internal standard) were stirred (600 rpm) at 90 ºC for the desired reaction time (CAUTION: the combination of air and H$_2$O$_2$ with organic compounds at elevated temperatures may be explosive!). In some runs under the optimized conditions, 2,2,6,6-tetramethylpiperidine-1-oxyl (TEMPO, 1.0 mmol) was added to the initial reaction mixture as a radical scavenger.

For a typical oxidation of cyclohexane: cyclohexane (5.0 mmol), hydrogen peroxide (30% w/w aq. sol., 10.0 mmol), 3 mL of acetonitrile, complex **1** or **2** (0.2 mol% vs. cyclohexane) and 50 μL of nitromethane (internal standard) were stirred (600 rpm) at 60 ºC for the desired reaction time (CAUTION: the combination of air and H$_2$O$_2$ with organic compounds at elevated temperatures may be explosive!). In some runs under the optimized conditions, the radical scavenger diphenylamine (10.0 mmol) was added to the initial reaction mixture.

Along the oxidation reactions, small aliquots were taken, cooled down, centrifuged (to separate the catalyst from the sample) and analysed by GC using the internal standard method for quantification. In the case of cyclohexane oxidation, prior to the GC analysis an excess of triphenylphosphine was added to reduce the formed cyclohexyl hydroperoxide to the corresponding alcohol, following a method developed by Shul'pin[12–15] (cyclohexyl hydroperoxide is transformed in the GC injector into a mixture of cyclohexanol and cyclohexanone. Thus, the reaction samples are quantitatively reduced with triphenylphosphine to obtain cyclohexanol. This method allowed to calculate the real concentrations not only of the hydroperoxide but of the alcohol and ketone present in the solution at a given moment). The GC analyses were carried out in a FISONS Instruments GC 8000 series gas chromatograph with a capillary DB-WAX column (30 m x 0.32 mm) and a FID detector under the following conditions: program 120 ºC for 1 min, 10 ºC/min, 200 ºC for 1 min, injector at 240 ºC and helium as the carrier gas. In addition, GC-MS analyses were conducted at a Perkin-Elmer Clarus 600 C apparatus, using He as the carrier gas, with an ionization voltage of 70 eV and a SGE BPX5 column (30 m × 0.25 mm × 0.25 μm). The identification of oxidation products was provided by comparison of the products retention times with those of known reference compounds. Their mass spectra fragmentation patterns were compared with those obtained from the NIST spectral library of the spectrometer computer software. The conversion values considered result from two concordant assays.

Blank reactions were performed for the best conditions in the absence of complexes **1** or **2**. They confirmed that almost no oxidation occurs in such conditions.

The recyclability of both complexes was examined, by recovering them by centrifugation after the reaction mixture being cooled down, washing with acetonitrile and drying in oven at 60 ºC overnight. Each new catalytic cycle was initiated after the preceding one with the recovered catalyst by addition of new typical portions of all other reagents. After completion of the reaction, the products were analysed as described above.

OPTIMIZATION OF THE CATALYTIC REACTION CONDITIONS

Table S1. Optimization conditions for the microwave-assisted oxidation of styrene to benzaldehyde, by hydrogen peroxide, catalysed by **1** for 30 min.

$n_{ox}/n_{styrene}$ /mol%	$n_1/n_{styrene}$ /mol%	MW power /W	MW rot /rpm	T /°C	Yield (%)	Select. /%	TOF (h^{-1})
2	1	10	600	60	31.7	80	63.4
2	1	15	600	60	43.2	82	86.4
2	1	20	600	60	46.0	87	92.0
2	1	10	600	75	37.2	88	74.4
2	1	15	600	75	46.2	93	92.4
2	1	20	600	75	50.1	93	100.2
2	1	10	600	90	52.7	100	105.4
2	1	20	600	90	59.7	100	119.4
2	1	15	600	90	59.9	100	119.8
2	1	15	800	90	60.1	100	120.2
2	1	15	800	75	50.2	86	100.4
2	1	15	800	60	44.1	76	88.2
3	1	15	600	75	39.8	61	79.6
3	1	15	600	90	31.3	54	62.6
3	1	15	800	90	27.4	52	54.8
2	0.5	15	600	90	38.5	94	77.0
2	1.5	15	600	90	61.2	92	122.4
2	1.5	15	600	75	49.2	81	98.4
2	2	15	600	90	36.4	67	72.8

Table S2. Optimization conditions for the microwave-assisted oxidation of cyclohexane to KA oil, by hydrogen peroxide catalysed by **1** for 2 h.

n_{ox}/n_{CyH} /mol%	n_1/n_{CyH} /mol%	MW power /W	MW rot /rpm	T /°C	Yield (%)	Select. /%	TON
2	0.5	10	600	50	27.8	92	55.6
2	0.5	10	600	60	35.3	87	70.6
2	0.5	10	800	60	35.7	81	71.4
2	0.5	15	800	60	29.8	77	59.6
2	0.2	15	600	60	37.1	>99	185.5
2	0.2	15	600	70	27.2	84	136.0
2	0.1	10	600	60	21.9	>99	219.0
2	0.1	10	600	70	28.2	91	282.0
2	0.15	15	600	60	30.0	>99	200.0
2	0.1	10	600	50	18.6	>99	186.0
2	0.2	10	600	60	36.9	>99	184.5
3	0.2	10	600	60	13.9	66	69.5
3	0.2	10	800	60	13.0	67	65.0
3	0.2	10	600	50	18.6	75	93.0
3	0.1	10	600	60	28.4	79	284.0
2	0.2	15	600	60	37.1	>99	185.5
2	0.2	20	600	50	34.7	>99	173.5
2	0.2	10	600	50	31.8	>99	159.0
2	0.2	20	600	70	28.8	82	144.0
2	0.2	15	800	60	34.5	98	172.5
2	0.2	10	800	60	36.3	>99	181.5
2	0.2	15	800	75	31.2	88	156.0
2	0.2	15	800	60	37.3	97	186.5

SOLUTION STUDIES

In order to carry out full physicochemical characterization of the studied ligands and their complexes with Cu(II) ions, including coordination model, a combination of physico-chemical methods, i.e. mass spectrometry, potentiometric titrations, absorption spectroscopy in the range of UV-Vis and EPR spectroscopy, was used.

Speciation studies.

The titrations of the solutions containing only the ligand were used to determine the protonation constants of the studied ligand (Table 1), which in the later steps were taken into account when calculating the cumulative stability constants βmhl of the complexes; the ligand and proton concentrations were determined from the Gran function.[6] The calculations for the results obtained from the potentiometric measurements were performed by Superquad program,[7] based on the iterative least squares method.[8]

The degree of fit of both experimental and theoretical curves as well as the values of standard deviations obtained during the calculations was the basis for the selection of the optimal model of both the protonation/complexation schemes and the stability constants values (in literature presenting solution speciation studies, potentiometric curves obtained from the titrations are presented very rarely, and therefore we have followed the usual practice not to show them). Based on the protonation and stability constants (Table 1), the species distribution profiles were visualized in the Hyss2009 program,[16] and presented in Figure 1 for complexation.

In literature presenting solution speciation studies, potentiometric curves obtained from the titrations are presented very rarely, and therefore we have followed the usual practice not to show them.
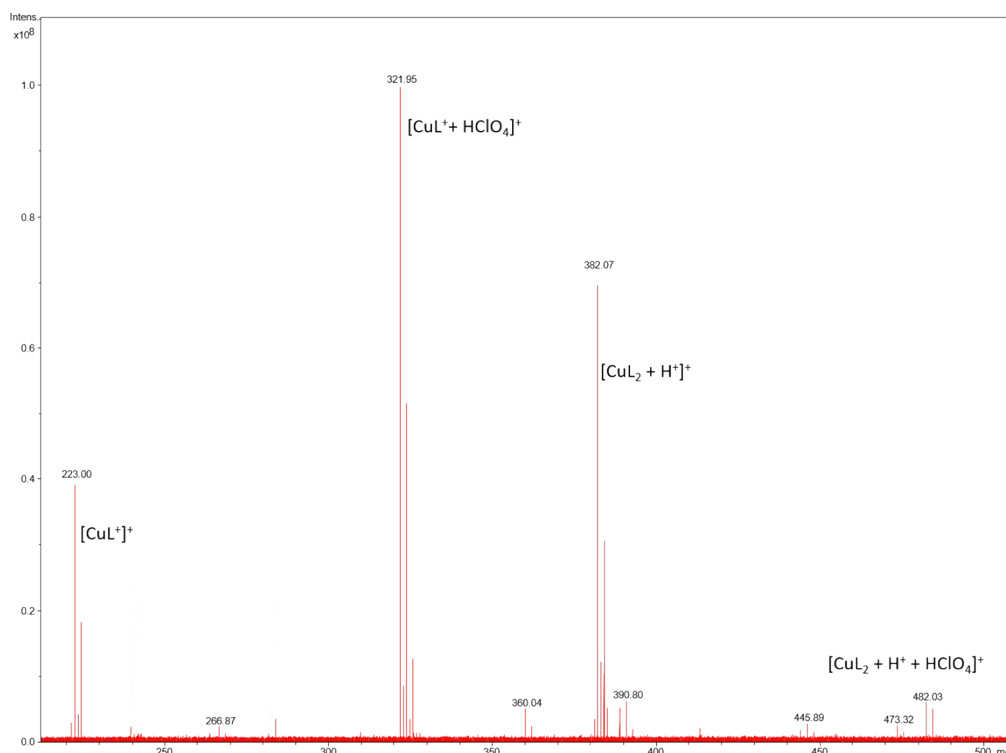
Stoichiometries of Cu(II) complexes.

Figure S4. ESI-MS spectra of the reaction mixture of Cu(II):HL, with a metal to ligand molar ratio of 1:1

Complex formation equilibria.

The proposal of species calculated in Cu(II)-L systems came from the analysis of pH-dependent variations of UV-Vis and EPR spectra. The pH-dependent UV-visible spectral profile of the Cu(II) – L complex as a function of pH, are shown in Figure S5 and spectra changes are presented in Table 1 and discussed in main manuscript.

The assignment of coordination species with the UV-Vis peaks was based on the comparison of the obtained distributions of complex forms with the obtained UV-Vis spectra, as well as on the literature data showing that an increase of the number of N-donors in the coordination sphere of copper ions, causes a hypsochromic shift of the observed bands.[17,18] At the same time, it should be remembered that the number and type of N donor atoms in the ligand structure, the presence of additional substituents that can inductively affect the donor groups and the position in the coordination sphere of the metal ion also affects the spectroscopic parameters.
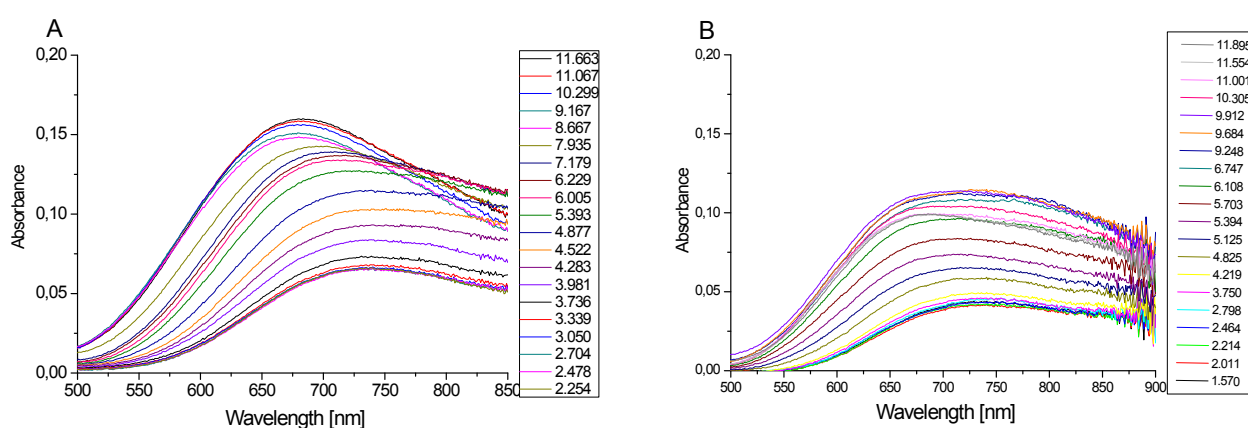

Figure S5. The UV-Vis spectra as a function of pH for Cu(II):HL systems. A: Cu(II):HL 1:1 molar ratio, $[Cu(II)] = [HL] = 2 \cdot 10^{-3}$ M; B: Cu(II):HL 1:3 molar ratio, $[Cu(II)] = 6.65 \cdot 10^{-4}$ M, $[HL] = 2 \cdot 10^{-3}$ M; $I = 0.1$M $NaNO_3$ 80:20 MeOH/H_2O (w/w).

EPR technique allowed to definitively observe an appearance of dimeric species (through the loss of EPR signal) above pH 7 (Figure S6), and an introduction of species with appropriate, dimeric, stoichiometry into the potentiometric calculations.
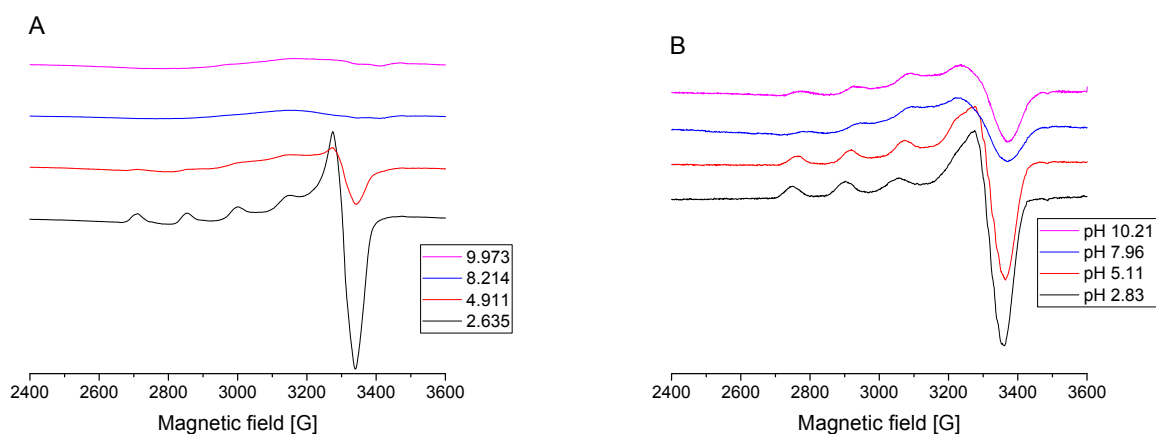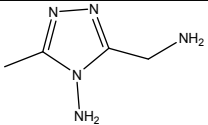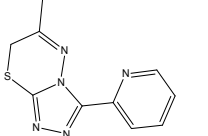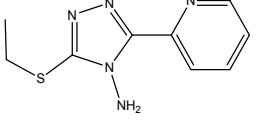
Figure S6. The EPR spectra as a function of pH for Cu(II):HL systems. A: Cu(II):HL 1:1 molar ratio, [Cu(II)] = [HL] = $2 \cdot 10^{-3}$ M; B: Cu(II):HL 1:3 molar ratio, [Cu(II)] = $6.65 \cdot 10^{-4}$M, [HL] = $2 \cdot 10^{-3}$ M; I = 0.1M NaNO$_3$ 80:20 MeOH/H$_2$O (w/w).

Table S3. Literature potentiometric and spectroscopic data for Cu(II) complexes of the selected ligands.

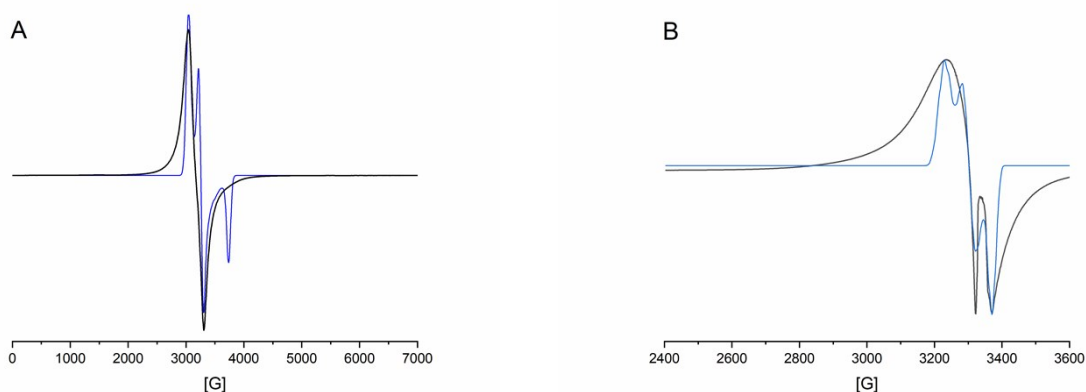| Ligand/Complexes		logβ	λ_{max} [nm]	ε [M^{-1}cm^{-1}]
	3-(aminomethyl)-5-methyl-4H-1,2,4-triazol-4-amine (A)			
	[CuL]$^{2+}$	6.47	708	40
	[CuL$_2$]$^{2+}$	12.34	594	61
	6-methyl-3-(pyridin-2-yl)-7H-[1,2,4]triazolo[3,4-b][1,3,4]thiadiazine (B)			
	[CuL]$^{2+}$	4.75		
	[CuL$_2$]$^{2+}$	9.72		
	3-(ethylthio)-5-(pyridin-2-yl)-4H-1,2,4-triazol-4-amine (C)			
	[CuL]$^{2+}$	4.62	736	35
	[CuL$_2$]$^{2+}$	8.61	660	55

Figure S7. The EPR spectra for A: complex **1**; B: complex **2.** Blue line represents the best fit.
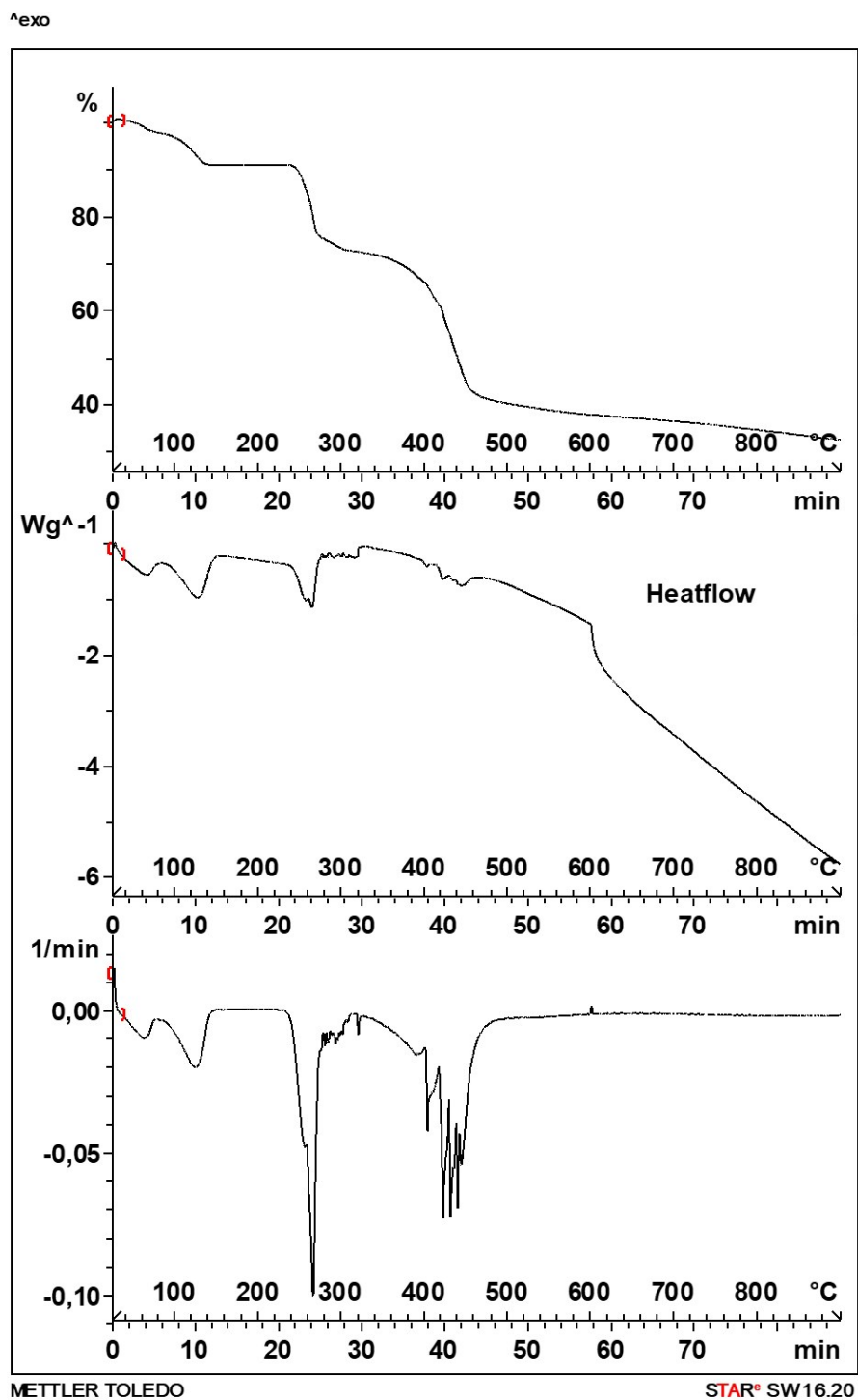
THERMAL ANALYSES
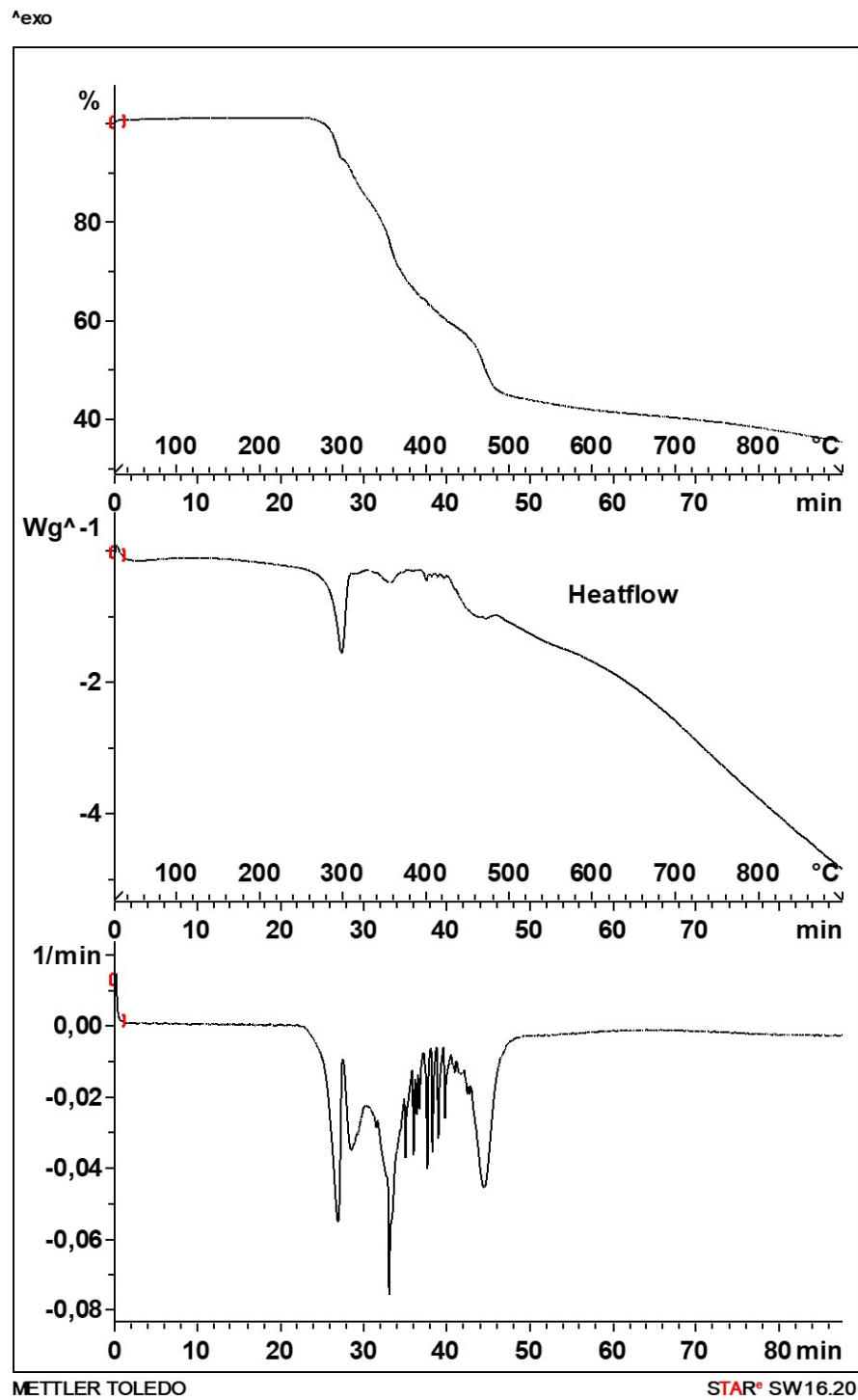

Figure S8. The TGA curves for complex **1**

Figure S9. The TGA curves for complex **2**

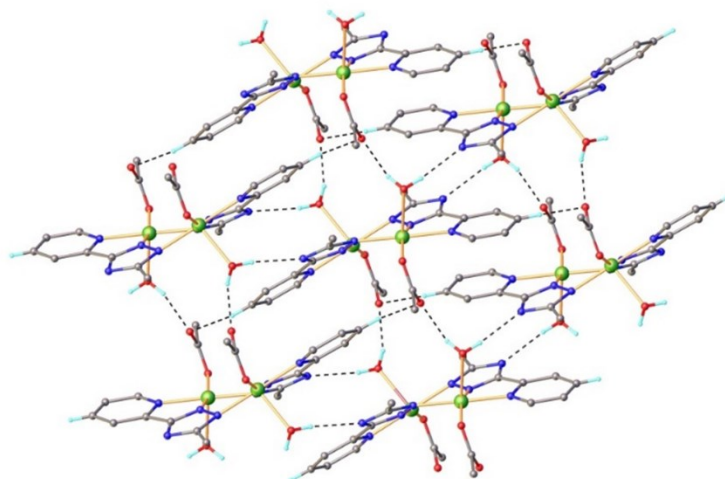# CRYSTAL DATA

Figure S10. 2D-supramolecular layer architecture in the crystal structure $[Cu_2(L)_2(OAc)_2(H_2O)_2]$ (**1**). H-atoms are not shown for clarity.
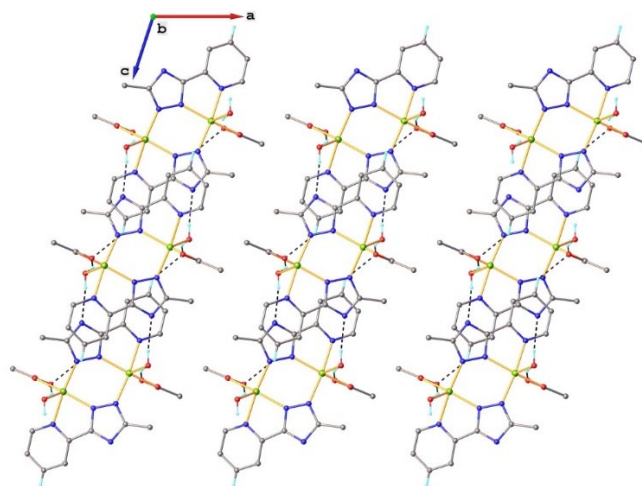

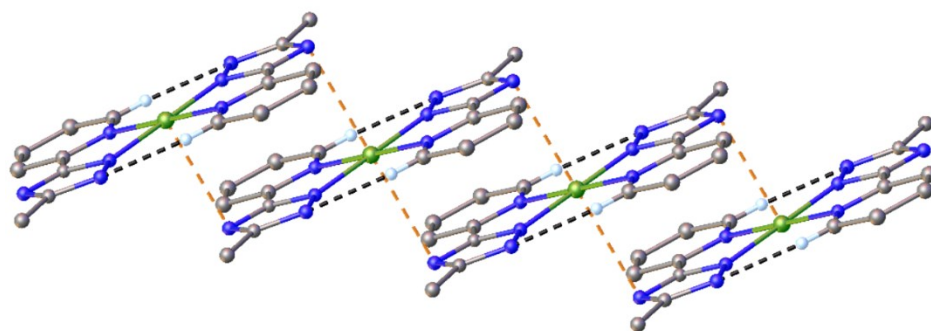**Figure S11.** Partial crystal packing in crystal **1** viewed along b axis.

CRYSTAL DATA

Figure S12. Ladder-like supramolecular architecture in the crystal structure **2**, H-atoms are not shown for clarity. Cu1···N4(1 + x, y, z) contacts are shown as dashed orange lines.

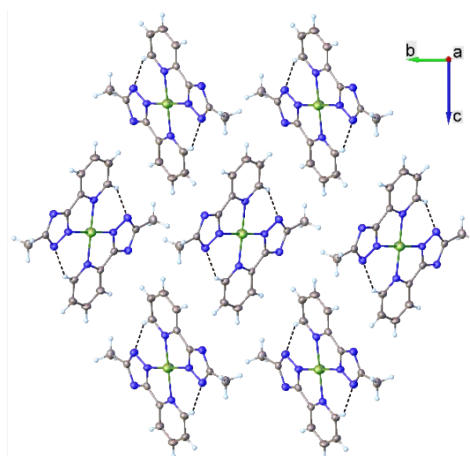**Figure S13.** Partial crystal packing in crystal **2** viewed along *a* axis.

Table S4. Bond lengths [Å] and angles [°] for **1**.

C1-C2	1.376(4)	N4-C1-C2	122.1(3)
C1-N4	1.335(4)	C3-C2-C1	119.7(3)
C2-C3	1.371(5)	C2-C3-C4	118.7(3)
C3-C4	1.378(4)	C5-C4-C3	119.0(3)
C4-C5	1.376(4)	C4-C5-C6	124.9(3)
C5-C6	1.468(4)	N4-C5-C4	122.3(3)
C5-N4	1.350(4)	N4-C5-C6	112.7(2)
C6-N1	1.325(4)	N1-C6-C5	117.1(3)
C6-N3	1.343(3)	N1-C6-N3	114.0(2)
C7-C8	1.492(4)	N3-C6-C5	128.8(3)
C7-N2	1.344(3)	N2-C7-C8	123.4(3)
C7-N3	1.346(3)	N2-C7-N3	112.9(2)
C9-C10	1.503(4)	N3-C7-C8	123.8(3)
C9-O1	1.273(3)	O1-C9-C10	116.4(3)
C9-O2	1.241(3)	O2-C9-C10	120.2(3)
Cu1-N1	1.999(2)	O2-C9-O1	123.4(3)
Cu1-N2[1]	1.989(2)	N1-Cu1-N4	79.92(9)
Cu1-N4	2.046(2)	N1-Cu1-O3	105.41(8)
Cu1-O1	1.966(2)	N2[1]-Cu1-N1	93.95(9)
Cu1-O3	2.289(2)	N2[1]-Cu1-N4	173.88(9)
N1-N2	1.372(3)	N2[1]-Cu1-O3	99.21(8)
		N4-Cu1-O3	82.56(8)
		O1-Cu1-N1	161.50(8)
		O1-Cu1-N2[1]	93.49(9)
		O1-Cu1-N4	92.36(9)
		O1-Cu1-O3	90.06(7)
		C6-N1-Cu1	113.71(19)
		C6-N1-N2	105.6(2)
		N2-N1-Cu1	139.29(18)
		C7-N2-Cu1[1]	132.25(19)
		C7-N2-N1	105.6(2)
		N1-N2-Cu1[1]	118.91(17)
		C6-N3-C7	102.0(2)
		C1-N4-C5	118.2(2)
		C1-N4-Cu1	127.5(2)
		C5-N4-Cu1	114.24(18)
		C9-O1-Cu1	114.17(18)

Symmetry code:[1]1−*x*,+*y*,0.5−*z*

Table S5. Bond lengths [Å] and angles [°] for **2**.

Cu1-N1	2.036(3)	N2-Cu1-N1[1]	98.67(11)
Cu1-N1[1]	2.036(3)	N2[1]-Cu1-N1	98.67(11)
Cu1-N2	1.946(3)	N2[1]-Cu1-N1[1]	81.33(11)
Cu1-N2[1]	1.946(3)	N2-Cu1-N1	81.33(11)
N1-C1	1.343(4)	C1-N1-Cu1	128.0(2)
N1-C5	1.346(4)	C1-N1-C5	118.2(3)
N2-N3	1.369(4)	C5-N1-Cu1	113.8(2)
N2-C6	1.329(4)	N3-N2-Cu1	138.6(2)
N3-C7	1.329(4)	C6-N2-Cu1	114.4(2)
N4-C6	1.332(4)	C6-N2-N3	106.6(3)
N4-C7	1.357(4)	C7-N3-N2	104.1(3)
C1-C2	1.380(5)	C6-N4-C7	100.8(3)
C2-C3	1.374(5)	N1-C1-C2	121.6(3)
C3-C4	1.373(5)	C3-C2-C1	119.6(3)
C4-C5	1.373(4)	C4-C3-C2	119.0(4)
C5-C6	1.464(5)	C5-C4-C3	118.9(4)
C7-C8	1.493(4)	N1-C5-C4	122.7(3)
		N1-C5-C6	112.4(3)
		C4-C5-C6	124.9(3)
		N2-C6-N4	113.9(3)
		N2-C6-C5	117.6(3)
		N4-C6-C5	128.5(3)
		N3-C7-N4	114.7(3)
		N3-C7-C8	122.3(3)
		N4-C7-C8	123.0(3)

Symmetry code:[1]2 −x, 1 −y,1−z

Table S6. H-bonds parameters for **1.**

D–H···A	Distance, Å			DHA angle, deg	Symmetry code for A
	D–H	H···A	D···A		
C1-H···O1	0.93	2.59	3.086(4)	114.1	*x, y, z*
C4-H···O2	0.93	2.53	3.347(4)	147.5	*1−x,1−y,−z*
C4-H···O3	0.93	2.60	3.429(4)	148.6	*1−x,2−y,−z*
O3-H3···O2	0.86	1.96	2.709(3)	146.3	*x ,1+y, +z*
O3-H3···N3	0.86	2.16	3.005(3)	170.7	*1−x,2−y,−z*

REFERENCES

1   O. D. Ltd, 2003.

2   O. V. Dolomanov, L. J. Bourhis, R. J. Gildea, J. A. K. Howard and H. Puschmann, *J. Appl. Crystallogr.*, 2009, **42**, 339–341.

3   G. M. Sheldrick, *Acta Crystallogr. Sect. C*, 2015, **71**, 3–8.

4   G. A. Bain and J. F. Berry, *J. Chem. Educ.*, 2008, **85**, 532–536.

5   O'Connor, *Prog. Inorg. Chem.*, 1982, **29**, 203–283.

6   G. Gran, *Acta Chem. Scand.*, 1950, 559–577.

7   P. Gans, A. Sabatini and A. Vacca, *J. Chem. Soc. Dalt. Trans.*, 1985, 1195–1200.

8   G. Peter, *Data fitting in the chemical sciences : by the method of least squares*, John Wiley & Sons, Ltd, 1992.

9   D. B. Rorabacher, W. J. Mackellar, F. R. Shu and S. M. Bonavita, *Anal. Chem.*, 1971, **43**, 561–573.

10   C. L. de Ligny, P. F. M. Luykx, M. Rehbach and A. A. Wieneke, *Recl. des Trav. Chim. des Pays-Bas*, 2010, **79**, 699–712.

11   C. L. de Ligny, P. F. M. Luykx, M. Rehbach and A. A. Wieneke, *Recl. des Trav. Chim. des Pays-Bas*, 2010, **79**, 713–726.

12   G. Shul'pin, *Catalysts*, 2016, **6**, 50.

13   G. B. Shul'pin, *J. Mol. Catal. A Chem.*, 2002, **189**, 39–66.

14   G. B. Shul'pin, *Comptes Rendus Chim.*, 2003, 6, 163–178.

15   G. B. Shul'Pin, Y. N. Kozlov, L. S. Shul'Pina, A. R. Kudinov and D. Mandelli, *Inorg. Chem.*, 2009, **48**, 10480–10482.

16   L. Alderighi, P. Gans, A. Ienco, D. Peters, A. Sabatini and A. Vacca, *Coord. Chem. Rev.*, 1999, 184, 311–318.

17   Pettit L.D., Gregor J.E. and H. Kozłowski, *Perspectives on Bioinorganic Chemistry*, London, JAI Press., 1999, vol. 1.

18   Kowalik-Jankowska T., Kozłowski H., Farkas E. and Sovago I., in *pubs.rsc.org*, eds. A. Sigel, Roland KO Sigel and Helmut Sigel, John Wiley & Sons, Ltd, 2007, vol. 2, pp. 63–108.